*Tellus (2008), 60B, 167–178*
*Printed in Singapore. All rights reserved*



**TELLUS**

# $H_2O$ and $CO_2$ fluxes at the floor of a boreal pine forest

*By* LIISA KULMALA[1]*, SAMULI LAUNIAINEN[2], JUKKA PUMPANEN[1], HARRY LANKREIJER[3], ANDERS LINDROTH[3], PERTTI HARI[1] and TIMO VESALA[2], [1]*Department of Forest Ecology, P.O. Box 27, FIN-00014, University of Helsinki, Finland;* [2]*Department of Physical Sciences, P.O. Box 64, FIN-00014, University of Helsinki, Finland;* [3]*Department of Physical Geography and Ecosystem Analysis, Lund University, Sölvegatan 12, 223 62, Lund, Sweden*

(Manuscript received 29 December 2006; in final form 14 September 2007)

ABSTRACT

We measured $H_2O$ and $CO_2$ fluxes at a boreal forest floor using eddy covariance (EC) and chamber methods. Maximum evapotranspiration measured with EC ranged from 1.5 to 2.0 mmol $m^{-2}$ $s^{-1}$ while chamber estimates depended substantially on the location and the vegetation inside the chamber. The daytime net $CO_2$ exchange measured with EC (0–2 $\mu$mol $m^{-2}$ $s^{-1}$) was of the same order as measured with the chambers. The nocturnal net $CO_2$ exchange measured with the chambers ranged from 4 to 7 $\mu$mol $m^{-2}$ $s^{-1}$ and with EC from ~4 to ~5 $\mu$mol $m^{-2}$ $s^{-1}$ when turbulent mixing below the canopy was sufficient and the measurements were reliable.

We studied gross photosynthesis by measuring the light response curves of the most common forest floor species and found the saturated rates of photosynthesis ($P_{max}$) to range from 0.008 (mosses) to 0.184 $\mu$mol $g^{-1}$ $s^{-1}$ (blueberry). The estimated gross photosynthesis at the study site based on average leaf masses and the light response curves of individual plant species was 2–3 $\mu$mol $m^{-2}$ $s^{-1}$. At the same time, we measured a whole community with another chamber and found maximum gross photosynthesis rates from 4 to 7 $\mu$mol $m^{-2}$ $s^{-1}$.

## 1. Introduction

Forest floor vegetation is usually assumed to play a small role in the carbon cycle and it is typically studied only as a part of soil flux measurements. However, some studies estimate that forest floor vegetation can momentarily assimilate as much as 50% (Goulden and Crill, 1997) of the total assimilated carbon in a closed canopy. Kolari et al. (2006) found that the annual gross photosynthesis of forest floor vegetation is 0.48 kg $CO_2$ $m^{-2}$ (13% the total ecosystem gross photosynthesis). Morén and Lindroth (2000) revealed that the annual gross photosynthesis of forest floor vegetation is 0.7 kg $CO_2$ $m^{-2}$ in a 70-year-old Norway spruce and Scots pine forest. Swanson and Flanagan (2001) found the forest floor vegetation to annually assimilate 0.51 kg $CO_2$ $m^{-2}$ in 120-years-old black spruce forest. The estimated amount of fixed carbon varies from site to site depending on climate, canopy structure and vegetation. For reliable estimates of net fluxes from large areas, we must understand the effects of different environmental variables on the capacity of vegetation and soil activity to bind and produce $H_20$ and $CO_2$.

Forest floor fluxes can be measured with different methods. One common method uses a transparent soil chamber which measures the net exchange of the forest floor: efflux from the soil and the net exchange of forest floor vegetation (e.g. Morén and Lindroth, 2000; Pumpanen et al., 2001). Another method used to measure the net forest floor exchange is the eddy covariance (EC) method. EC is a direct micrometeorological method that measures the energy and gas exchange between the underlying surface and the atmosphere '*in situ*' without disturbing the system, and is routinely used in flux measurements above various ecosystems, such as forests (Baldocchi, 2003). Recently, this method has yielded good results when used below the forest canopy to measure the net energy and mass exchange between the forest floor and the atmosphere (Blanken et al., 1998; Baldocchi et al., 2000; Wilson and Meyers, 2001; Launiainen et al., 2005; Misson et al., 2007). With EC, one can in favourable conditions measure average net exchange over an area from hundreds to thousands of times larger than the source area of a chamber measurement. Different methods used for estimating the photosynthesis and respiration of the vegetation may yield different estimates to the contribution of forest floor vegetation to the carbon budget.

The aim of this study was to quantify the $H_2O$ and $CO_2$ fluxes from soil and forest floor vegetation on an ecosystem scale and to compare the results with those of earlier studies. We measured the net $CO_2$ exchange, the sum of soil $CO_2$ efflux and the gas exchange of forest floor vegetation with EC and two different chamber methods: the closed dynamic chamber system and an

*Corresponding author.
e-mail: liisa.kulmala@helsinki.fi
DOI: 10.1111/j.1600-0889.2007.00327.x

open dynamic chamber (Pumpanen et al., 2001). Photosynthesis of the most common forest floor species was measured with a closed static chamber. Evapotranspiration was measured with EC and the closed dynamic chamber.

## 2. Materials and methods

### 2.1. Study site and estimation of forest floor vegetation

The measurements were carried out at SMEARII station in Hyytiälä (Hari and Kulmala, 2005) in southern Finland (61.52 N, 24.17 E). The study site comprised 45-year-old Scots pine stand. The soil at the site was exposed to prescribed burning and ploughing before sowing in 1962. In summer 2005, the dominant height of the stand was 16 m, the tree density 1100–1200 $ha^{-1}$ and the total LAI ~7 $m^2$ $m^{-2}$. Lingonberry (*Vaccinium vitis-idaea*), blueberry (*Vaccinium myrtillus*) and mosses, mainly *Pleurozium schreberi* and *Dicranum polysetum dominated* the forest floor vegetation is dominated. According to the Finnish forest site type classification (Cajander, 1926), the forest belongs to the Vaccinium site type. The mean depth of the organic layer was 5.4 cm and the density, 0.13 g $cm^{-3}$. During the period from 1960 to 1990, the annual mean temperature was +2.9 °C and precipitation, 709 mm. January was the coldest month (mean −8.9 °C) and July, the warmest (mean +15.9 °C).

We estimated the average forest floor biomass at the study site by systematically collecting 80 aboveground samples of forest floor vegetation from an area of 12.6 ha. The samples were collected at 20-metre intervals along eight lines starting from the eddy tower and directed to cardinal points. One sample was 0.053 $m^2$ in size. We separated each sample into different species, and each species into leaves and stem. From mosses, we separated the green parts. We then weighed the different segments after drying in 60 °C for 24 h.

### 2.2. Net flux measurements

*2.2.1. Closed dynamic chamber (Big chamber).* The automated chamber was designed for measuring fluxes of $CO_2$ and $H_2O$ from the soil and forest floor vegetation under light and dark conditions, respectively. The size of the chamber was 0.30 × 0.58 × 0.58 m (height × width × length), and it was open upwards and downwards, towards the ground. The surface area of the forest floor in the chamber was 0.336 $m^2$. The lower end of the chamber consisted of a sharp aluminium frame which was firmly pressed a few centimetres into the humus layer.

The basic structure of the chamber consisted of an aluminium frame covered with plexiglass on three sides and aluminium on one side. The chamber was always oriented with the dark side towards the north to prevent shading of the soil and forest floor vegetation. A fan was placed inside the chamber to mix the air during measurements. $H_2O$ and $CO_2$ concentrations were measured with a LI-COR 6262 IR-gas analyser (LI-COR, Inc. Lincoln, NE, USA) in absolute mode. In addition, a JYP 1000 PAR sensor (SDEC, France) measured photosynthetically active radiation (PAR) inside the chamber. Transparent chamber was darkened with by a darkening apparatus operated automatically and controlled by the software in the data logger. The fluxes of $CO_2$ and $H_2O$ were measured twice hourly by closing a lid of transparent plexiglass for 5 minutes. The lid opened after every measurement for a couple of minutes to allow ventilation to ambient concentrations. After ventilation, the lid was closed again and immediately thereafter the darkening apparatus was automatically positioned such that the whole chamber was covered in complete darkness. The flux was again measured over a five-minute period by measuring the rate of change in $H_2O$ and $CO_2$ concentrations.

The $H_2O$ and $CO_2$ concentrations were recorded every 10 seconds while the chamber was closed. The rate of change in concentrations was used to estimate the net flux. The air sampling system is made such that air is sucked through an approximately 200-cm-long tube perforated with ten small holes and which runs along the sides of the chamber. The air then goes to the gas analyser, through the pump and then back to the chamber. The flow rate is about 2 L $h^{-1}$.

The net flux of $CO_2$ and $H_2O$ were calculated from the time derivative of respective concentration ($dC_s/dt$). The $dC_s/dt$ is estimated as the slope of the linear regression through concentration readings from 50 to 200 seconds. The suppression of respiration in light is assumed to stop instantly in the dark and that a period of at least 15 minutes with the chamber open between the last dark and the next light reading was sufficient to suppress respiration again upon closure of the transparent lock. Flux estimates were used only if the regression line through the concentration readings had high linearity, indicated by an $R^2$ over 0.98. Such high linearity of the readings indicated a sufficient mixing of the air, low leakage and correct air sampling.

The momentary gross photosynthesis of the forest floor vegetation ($P_{ch}$) was determined from the difference between the $CO_2$ fluxes in the darkened and in the light chamber. The pair of light and dark measurements was repeated every 30 minutes.

We used the automatic chamber in three different locations during three different time periods (2–9 July, 2–9 August and 13–17 August 2005). The first measuring location was dominated by blueberry, and the second by lingonberry. Under these small woody dwarf shrubs, the ground was covered mainly with mosses. The third plot was dominated by mosses.

*2.2.2. Open dynamic chamber (Small chamber).* We also measured the net $CO_2$ flux from the forest floor with another automatic chamber system described in detail by Pumpanen et al. (2001). The chamber was transparent, 0.20 m in height and 0.19 m in diameter, providing a surface area of 0.028 $m^2$. The chamber was closed approximately once every hour for 3 minutes for the measurements. During the closure time, air was drawn out of the chamber at a flow rate of 4 L $min^{-1}$ and compensation air with known $CO_2$ concentration was simultaneously

introduced into the chamber at similar flow rate. The flux was determined from the flow rate and from the concentration differences between the inflow and outflow (Pumpanen et al., 2001).

During the campaign, the small chamber remained in the same location about 20 m away from the large chamber. The small chamber measured the temporal variation of fluxes at one spot, whereas the location of the large chamber was changed three times in order to measure different vegetation types and, thus, possible spatial variation. The flora in the small chamber was similar to, trough somewhat sparser than, the forest floor vegetation on the study site. The vegetation in the chamber consisted of mosses and some blueberry shoots.

*2.2.3. Eddy covariance measurements.* We measured the $CO_2$ and $H_2O$ fluxes with the EC method at a 3 m height of above the forest floor. The distance to the nearest trees ranged from 2 to 3 m depending on the direction. The wind field was measured with a 3-D sonic anemometer (USA-1, Metek GmbH, Elmshorn, Germany), and the mixing ratios with a closed-path infrared gas analyser (Li-Cor LI-7000, Li-Cor Inc, Lincoln, NE, USA) at 10 Hz frequency. The analogue signals from the gas analyser were collected into the analogue inputs of the sonic anemometer for synchronisation, and the data were stored for later post-processing. We then calculated the fluxes with standard methods (Aubinet et al., 2000). We applied 2-D co-ordinate rotation to the wind components and calculated the fluctuations in vertical wind ($w'$) and mixing ratios ($s'$) by removing linear trends from the data. The vertical fluxes of $CO_2$ and $H_2O$ were calculated, respectively, as:

$$F_{\mathrm{EC}} = \frac{p}{R\overline{T}}\overline{w'c'} \tag{1}$$

$$E_{\mathrm{EC}} = \frac{\overline{p}}{R\overline{T}}\overline{w'q'}, \tag{2}$$

where $F_{\mathrm{EC}}$ is the $CO_2$ flux ($\mu$mol m$^{-2}$ s$^{-1}$), $E_{\mathrm{EC}}$ the water flux (mmol m$^{-2}$ s$^{-1}$), $p$ the atmospheric pressure, $R$ the universal gas constant, $T$ the mean absolute temperature and $c'$ and $q'$ the fluctuations in $CO_2$- and $H_2O$ -mixing ratios, respectively. The over-bar denotes time averaging over the 30-minute period. We define the upward fluxes as positive, thus representing gain by the atmosphere. In calm conditions, the measured values do not necessarily represent the actual exchange between the surface and the atmosphere (Goulden et al., 1996; Aubinet et al., 2000). Consequently, we removed all periods when further analysis revealed a standard deviation of vertical wind speed ($\sigma_w$) of less than 0.11 m s$^{-1}$ (Launiainen et al., 2005). Unfortunately, the nights were very calm during the first half of the measurement period, so we had to ignore most of the nocturnal $F_{\mathrm{EC}}$ measurements. The source area for the EC fluxes depends on the prevailing conditions in the atmospheric surface layer. In near-neutral conditions, 80% of the fluxes measured at 3 m above the surface originate from the nearest 50 m in the upwind direction (Launiainen et al., 2005). The effect of stratification on within-canopy flux footprints is difficult to quantify, but qualitatively, the size of the source area increases slightly in stable and decreases in unstable stratification. Our results from multilayer subcanopy EC measurements of $H_2O$ and $CO_2$ fluxes (Launiainen et al., 2006), however, showed no significant variability with height. In practice, this means that the mean characteristics of overlapping source areas of different sizes did not substantially vary at the site. A single EC setup is therefore capable of measuring the average exchange over an area large enough to compensate for the small-scale spatial heterogeneities. Launiainen et al. (2005) describe the subcanopy EC measurements at the site of this study in more detail and discuss the use of the method in trunk space.

### 2.3. The $CO_2$ gross photosynthesis of individual plant species

*2.3.1. Photosynthetic activity of dwarf shrubs.* We measured the light response curves for the photosynthesis of the most common vascular plant species of forest floor vegetation (i.e. lingonberry (*Vaccinium vitis-idaea*), blueberry (*Vaccinium myrtillus*) and heather (*Calluna vulgaris*)). The measurements were taken in 2-week intervals at the study site with a manual, cylindrical chamber based on the closed static chamber technique. The chamber used in the measurements was made of 5 mm transparent plexiglass and was 0.30 m in diameter, 0.40 m in height and open downwards, towards the ground. During the measurements, the chamber was placed on a polyvinylchloride collar which was perforated to allow air to circulate freely under the chamber. Between the collar and the chamber was a 1-cm-thick sheet of cellular plastic. Shoots entered the chamber through a cut in the plastic, thus enabling us to measure the same shoots several times in their natural growing environment without changing the environmental factors or disturbing the shoots. We measured three individual lingonberry and blueberry shoots and two heather shoots. We varied the measurement order from shoot to shoot, but carried out all of the measurements between 8:00 and 18:00.

During the measurement, the $CO_2$ concentration inside the chamber was monitored with a novel $CO_2$ probe attached to the inside of the chamber based on the NDIR technique (GMP343, Vaisala Corporation, Vantaa, Finland). The $CO_2$ concentration readings were recorded at 5-second intervals and corrected automatically for humidity, temperature and pressure with a data recorder (MI70, Vaisala Corporation, Vantaa, Finland). The humidity and temperature values used for correction were obtained from a temperature and humidity probe (HMP75, Vaisala Corporation, Vantaa, Finland) attached to the inside of the chamber and connected to the MI70 data recorder. A small fan was used to mix the air inside. The intensity of PAR was measured with a PAR sensor (LI-190, LI-COR Biosciences, Lincoln, USA) attached to the outside of the chamber. Atmospheric pressure used for correcting measured $CO_2$ concentration values was monitored at the SMEARII station.

One set of measurements consisted of four to six repetitions with different light intensities and one dark measurement. The

highest light intensity was direct sunlight and the other four to five light intensities were created by shadowing the chamber with layers of netted fabric. During the dark measurement, the chamber was fully darkened with an aluminium cover. After the measurements, the aboveground parts of the measured plants were collected, dried for 24 hours at 60 °C and weighted in order to measure the leaf biomass.

For each set of measurements, we fitted a Michaelis–Menten-type equation to the data as follows:

$$P_{\mathrm{i}}(t) = \frac{P_{\mathrm{max_i}} I(t)}{b_{\mathrm{i}} + I(t)} \tag{3}$$

In the equation, $P_{\mathrm{i}}$ is the rate of gross photosynthesis per leaf mass ($\mu$mol g$^{-1}$ s$^{-1}$) of individual plant species $i$ (mosses, lingonberry, blueberry and heather), $I$ is the momentary intensity of PAR ($\mu$mol m$^{-2}$ s$^{-1}$), $P_{\mathrm{maxi}}$ is the rate of light saturated gross photosynthesis of an individual plant species per leaf mass (i.e. photosynthetic activity), and $b_{\mathrm{i}}$ ($\mu$mol g$^{-1}$ s$^{-1}$) is the species-specific light intensity when the gross photosynthesis rate is half the rate of light-saturated gross photosynthesis. We measured several individual shoots of different species and scaled the shoot-specific $P_{\mathrm{max}}$ values by leaf mass. In further analysis, we used an average of the parameters determined separately for each plant species.

*2.3.2. Photosynthetic activity of mosses.* We measured the gross photosynthesis of mosses with a chamber similar to the small chamber. We removed patches of *Pleurozium schreberi* and *Dicranum polysetum* from the soil 1 month before the campaign and placed them on quartz sand in order to separate the respiration and photosynthetic signal of the mosses from the soil $CO_2$ efflux. $CO_2$ efflux from the quartz sand was smaller and remained more constant over 24 hours in this artificial soil than in natural soil because of the absence of decomposing soil organic matter or root and rhizosphere respiration. The patches on the sand substrate were placed on the forest floor in their natural temperature, humidity and light environment.

The chamber measured $CO_2$ exchange approximately 60 times per day. PAR and temperature were monitored during the measurement. The green parts of the mosses were dried and weighed after the measurement campaign and a Michaelis–Menten-type light response curve similar to that of the dwarf shrubs (eq. 3) was fitted to the measurements of each day. From the daily $P_{\mathrm{max}}$ values we calculated one average value for each measurement period. During the first measuring period (2–9 July), no moss measurements were made, and therefore for this period we used average parameters from measurements taken 25–27 June and 12–14 July.

*2.3.3. Upscaling the gross photosynthesis of forest floor vegetation.* We used the PAR measurements from the big chamber, average leaf biomass and the photosynthetic light response parameters of each plant species from different periods to estimate the momentary rate of gross photosynthesis ($P_{\mathrm{e}}$) for the forest floor vegetation at the study site. Momentary $P_{\mathrm{e}}$ was calculated with the following equation:

$$P_{\mathrm{e}}(t) = \sum_i m_i P_{\mathrm{i}}(I(t)), \tag{4}$$

where $i$ is the species measured (mosses, lingonberry, blueberry and heather), $m_{\mathrm{i}}$ is the average leaf mass estimated from the systematic sampling, $P_{\mathrm{i}}$ is the light response curve for each species (eq. 3) and *I(t)* is the momentary PAR intensity. In addition, we used the same equation to estimate the momentary rate of gross photosynthesis in the big chamber ($P_{\mathrm{e\_ch}}$). In this case, $m_{\mathrm{i}}$ was the aboveground leaf biomass in the big chamber.

## 3. Results and discussion

### 3.1. Aboveground biomass

Blueberry and lingonberry dominated the dwarf shrub vegetation in the study site. The average aboveground biomasses of blueberry and lingonberry were 24 and 37 g m$^{-2}$, respectively, and that of the green parts of the mosses was 45 g m$^{-2}$. The total aboveground biomass was 124 g m$^{-2}$ (Table 1). The three measurement locations of the big chamber differed in their species composition (Table 1). The first plot contained a dense population of blueberry, but unfortunately no exact information was available on the biomasses. The second plot contained a dense lingonberry population; the biomass of the lingonberry was 146 g m$^{-2}$, and the total biomass 360 g m$^{-2}$, nearly three times that of the average forest floor vegetation. Moss populations with some lingonberry and blueberry shoots (Table 1) dominated the third plot. The total biomass (247 g m$^{-2}$) in the third plot was again much greater than the average, even though the biomasses of blueberry and lingonberry did not differ substantially from the average.

### 3.2. Weather conditions

The weather was mainly sunny during the first and the third measurement periods. During the second period the weather was cloudy except for 6 (sunny) and 7 August (partly cloudy). Rain fell intermittenly during the second period: On 4 August,

*Table 1.* The average above ground biomass (g m$^{-2}$) of different forest floor species at the study site and in the second and third locations of the big chamber (g m$^{-2}$). Blueberry dominated the first location of the big chamber, but the detailed information does not exist

| | Above ground biomass (g m$^{-2}$) | | | | | |
|---|---|---|---|---|---|---|
| | Blueberry | Lingonberry | Heather | Mosses | Others | Total |
| Average | 24 | 37 | 2 | 45 | 16 | 124 |
| 2nd plot | 61 | 146 | 0 | 152 | 1 | 360 |
| 3rd plot | 47 | 31 | 0 | 168 | 0 | 247 |

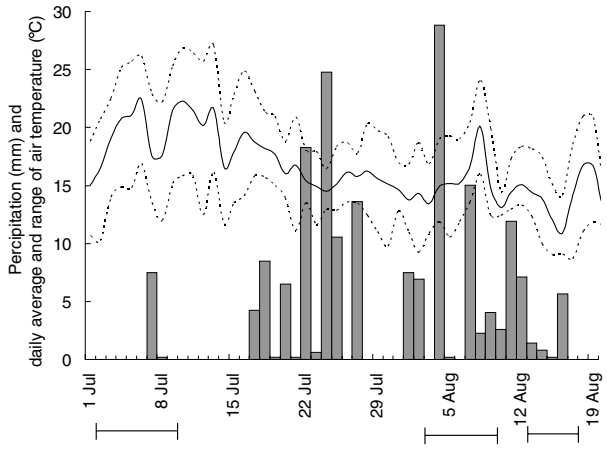


*Fig. 1.* Average (solid line), minimum and maximum (dashed lines) daily temperatures and percipitation (bars) from 1 July to 17 August 2005. The dates of the three measuring periods are shown with line segments.

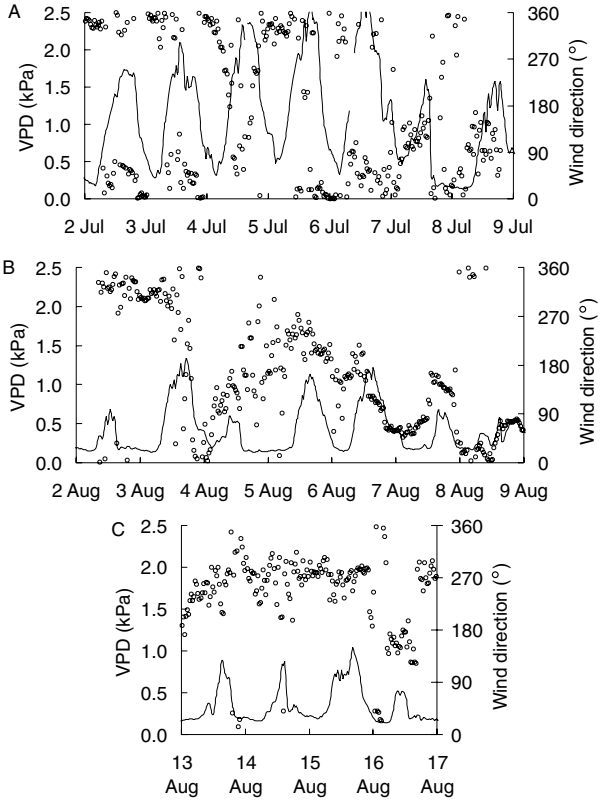


*Fig. 2.* Half-hourly average vapour pressure deficit (VPD) (kPa, solid line) and wind directions (°, circle) during the three measuring periods. The different panels (A, B, C) correspond to the different measuring periods.

precipitation was 29 mm, and on 7 Jul, 15 mm (Fig. 1). During the first and third measuring periods there were some light showers. The minimum air temperatures of all measurement periods were quite similar, around 8 °C, while the daily average temperatures (19, 15, 14 °C, respectively) and the maximum temperatures (27, 24, 19 °C, respectively) decreased (Fig. 1). Vapour pressure deficit (VPD) and wind direction during the three measurement periods appear in Fig. 2. Maximum VPD varied daily from 1.5 to 2.5 kPa during the first period and from 0.5 to 1 kPa during the later periods. In the first period, the wind was almost constantly northern, except for easterly wind on 7 June. In the second period, the wind was north-west during the first two days (2 and 3 August), and then turned to east on the third day (4 August). At the end of the period, the wind turned from the southwest (5 August) to the north (8 August). During the third period there was constantly western wind.

### *3.3. Net forest floor $H_2O$ exchange*

The evapotranspiration measured with the EC technique ($E_{ec}$) and the big chamber ($E_{ch}$) were of the same order of magnitude during the first seven measuring days (2–9 July), reaching a daytime maximum of 1.5–2.0 mmol $m^{-2}$ $s^{-1}$ (Fig. 3). During the second period (2–9 August), after the chamber was moved to a new position, $E_{ec}$ remained roughly at the same level (1.0–2.0 mmol $m^{-2}$ $s^{-1}$) as during the first period. The wind turned from the southwest to the north at the same time as the amplitude of the diurnal pattern decreased from 5 to 9 August. $E_{ch}$, on the other hand, was significantly lower with a daytime maxima ranging from 0.2 to 1.0 mmol $m^{-2}$ $s^{-1}$ during the whole measurement period (Fig. 3.). Because $E_{ec}$, which represents the average forest floor evapotranspiration, remained at nearly the same level as before, the substantial decrease in $E_{ch}$ was most likely due to the different vegetation inside the chamber, rather than to changes in the environmental conditions. The difference in evapotranspiration rates was presumably attributable to dominance of lingonberry at the second measurement location (Table 1). Lingonberry has adapted to drier environments and its transpiration rate is therefore lower than that of blueberry. The difference between the chamber and EC methods was somewhat smaller during cloudy days than during sunny days, which may be attributable to the shade-adaptation of lingonberry. Intermittent rain (Fig. 1) fell on the overcast days (low E).

During the third period (13–17 August), $E_{ec}$ was roughly 30% lower (1.0–1.5 mmol $m^{-2}$ $s^{-1}$) than during the previous periods. This decrease results presumably from low temperatures (Fig. 1) and low VPD (Fig. 2). The changes in wind direction (Fig. 2) have most likely minor effect since the vegetation is rather homogenous around the EC tower. Although $E_{ec}$ had decreased, it was still nearly double the $E_{ch}$ (Fig. 3.) of its new, moss-dominated location. This difference can be attributed to differences in vegetation, as was the case at the second location. Due to the lack of a vascular system and roots, the transpiration of the mosses (*Pleurozium schreberi* and *Dicranum polysetum*) is not controlled by the degree of stomatal opening or rate of

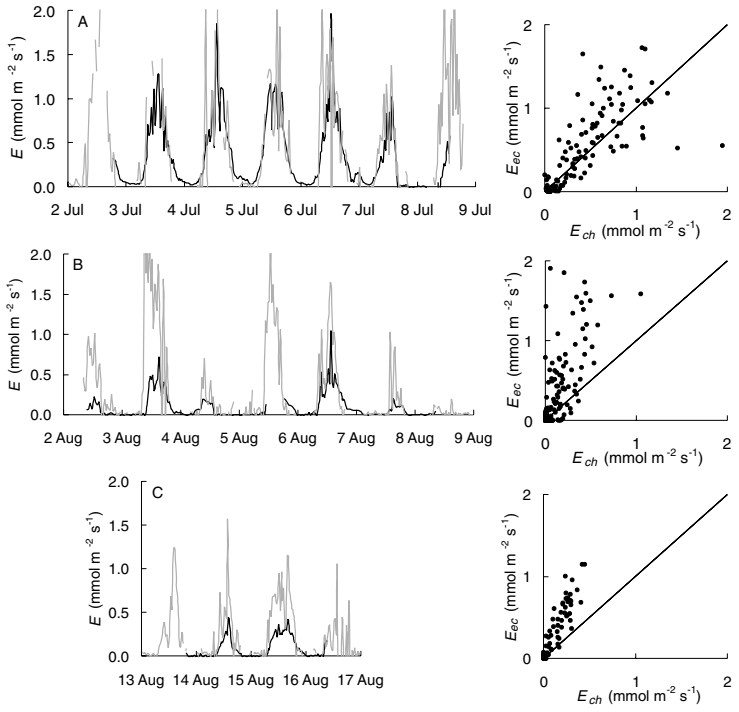


*Fig. 3.* Evapotranspiration measured with the big chamber ($E_{ch}$, black line) and with the eddy covariance (EC) method ($E_{ec}$, grey line). The different panels (A, B, C) correspond to the different measuring locations of the big chamber. The right hand side shows comparisons between $E_{ch}$ (x-axis) and $E_{ec}$ (y-axis).

gross photosynthesis, but depends mainly on the environmental conditions such as VPD, the water content of the mosses themselves, and the energy available for evaporation. Moreover, the leaf area per square meter of ground was smaller than that of the locations covered with shrub vegetation. Consequently, the transpiring leaf surface area was also smaller than that of the shrub-dominated locations. Furthermore, later in the season, when the angle of sun angle decreases, the shading of the chamber structure becomes more pronounced and may further reduce $E_{ch}$.

Our results are comparable to those of previous studies reporting forest floor evapotranspiration. Heijmans et al. (2004), who found evopotranspiration rates between 0.5 and 1.5 mmol $m^{-2}$ $s^{-1}$ for forest floor vegetation type of 'vascular plants', which consisted, for example of lingonberry and bog bilberry (*Vaccinium uliginosum)*. Constantin et al. (1999) used the EC method and measured maximum evapotranspiration rates between 0.8 and 1.4 mmol $m^{-2}$ $s^{-1}$ from the floor of a boreal mixed spruce and pine forest. Baldocchi and Vogel (1996) reported forest floor evapotranspiration rates averaged over several days. They found that the mean maximum E was around 1.1 mmol $m^{-2}$ $s^{-1}$ in a boreal Jack pine forest, but roughly half that in a temperate deciduous forest.

### *3.4. Net forest floor $CO_2$ exchange*

The nocturnal net $CO_2$ exchanges measured with the two automated chamber systems were comparable (∼5.0–6.0 $\mu$mol $m^{-2}$ $s^{-1}$) during the first measuring period, but the daytime values differed somewhat during some days (Fig. 4). Differences can be attributed largely to differences in vegetation. The largest diurnal amplitude of the net exchange was ∼6 $\mu$mol $m^{-2}$ $s^{-1}$ in the big chamber and ∼2.5 $\mu$mol $m^{-2}$ $s^{-1}$ in the small chamber. However, the diurnal patterns between these different chambers were similar even though they contained different vegetation. The daytime net forest floor exchange measured with the EC method ($F_{ec}$, 0–1 $\mu$mol $m^{-2}$ $s^{-1}$) is of the same order of magnitude as that measured with the big chamber. We had to ignore most of the nighttime values due to weak turbulent mixing, and therefore cannot estimate the diurnal pattern based on EC measurements.

The net $CO_2$ exchange measured with the small chamber became more positive during the second period because of increasing respiration resulting from rising soil temperatures (not shown). The big chamber, which had been relocated, showed values similar to those of first period (Fig. 4). The daytime $F_{ec}$ was of the same order of magnitude as that of the big chamber and had not changed since the first period. The nights were windier during the second measurement period which provided better conditions for EC measurements than during the first measurement period. The nocturnal data were in line with the chamber measurements, which showed increased net efflux (∼4–5 $\mu$mol $m^{-2}$ $s^{-1}$) during the nighttime. The difference between the chamber and EC estimates began to increase toward the end of the period.

In the third measurement location, the net $CO_2$ exchange measured with the big chamber was more positive than in previous locations (maximum nocturnal values ∼7.0 $\mu$mol $m^{-2}$ $s^{-1}$). The

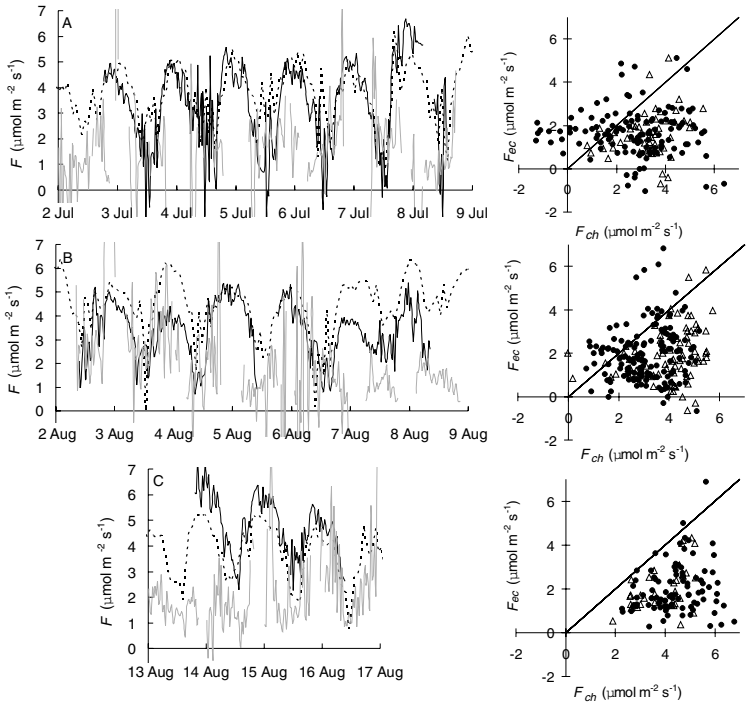


*Fig. 4.* Net $CO_2$ exchange between the forest floor and the atmosphere, measured with the EC (grey line), big chamber (black line) and small chamber (dashed line) methods. The different panels (A, B, C) correspond to the different measuring locations of the big chamber. The right hand side shows comparisons of the net $CO_2$ exchange measurements between the chamber ($F_{ch}$) and EC methods ($F_{ec}$). The big chamber is marked with black spheres and the small chamber, with triangles.

EC estimates and the small chamber values remained at the same level as in the second period, indicating no significant temporal variation. The different level of the nighttime net $CO_2$ exchange in the big chamber compared to that of the previous location indicates spatial variation in soil respiration. The different estimates became more concomitant during last two days of the third period (Fig. 4.). The difference between nocturnal and daytime values ($\sim 3\,\mu$mol m$^{-2}$ s$^{-1}$) was quite similar in both of the chambers. EC provided a similar daily cycle toward the end of the period when conditions were favourable for EC measurements. In general, the chambers showed more positive net $CO_2$ exchange than did the EC (Fig 4).

Our results are similar to those of other studies. Heijmans et al. (2004) found the net daytime $CO_2$ exchange for a forest floor dominated by vascular plants to vary between $-0.5$ and $1.5\,\mu$mol m$^{-2}$s$^{-1}$. Several authors have reported, based on EC measurements, net $CO_2$ exchanges between the forest floor and the atmosphere ranging from 0 to $5\,\mu$mol m$^{-2}$ s$^{-1}$ in boreal forests (Baldocchi and Vogel, 1996; Constantin et al., 1999; Subke and Tenhunen, 2004; Launiainen et al., 2005; Misson et al., 2007). Other studies have also found that mosses play an important role in the net $CO_2$ exchange of the forest floor. Goulden and Crill (1997) and Kolari et al. (2006) showed that the gross photosynthesis of mosses of mainly *Pleurozium schreberi* reduced the net $CO_2$ exchange by 0.5–1.0 $\mu$mol m$^{-2}$ s$^{-1}$. Janssens et al. (2001) and Swanson and Flanagan (2001) found other feather mosses to exhibit have photosynthesis of the same order of magnitude. Williams and Flanagan (1998) and Whitehead and Gover (2000) showed even higher values for the gross photosynthesis of *Pleurozium schreberi*, ranging between 1 and $2\,\mu$mol m$^{-2}$ s$^{-1}$. During the daytime, mosses in our big chamber reduced the exchange of $CO_2$ by more than $2\,\mu$mol m$^{-2}$ s$^{-1}$, but the moss population in the chamber was denser than that at the study site (Table 1). Although all of the other studies have been arranged in the boreal zone, comparison of our results to those of other studies is difficult given the differences in environmental conditions, such as the substrate or the age of the forests.

### 3.5. *Different components of $CO_2$ flux*

*3.5.1. Soil $CO_2$ flux and respiration of forest floor vegetation, $F_r$.* Figure. 5 shows the daily pattern of the aggregate soil $CO_2$ efflux and respiration of forest floor vegetation ($F_r$) and the soil temperature at a depth of 5 cm. $F_r$ was measured in the fully darkened big chamber. At the first location, the daily pattern of $F_r$ followed that of the soil temperature. During that period, respiration varied between 4 and $7\,\mu$mol m$^{-2}$ s$^{-1}$, being smallest in the early morning and highest in the late evening. On 7 July there was 8 mm of precipitation (Fig. 1.). After the rainfall, $F_r$ increased by $\sim 1\,\mu$mol m$^{-2}$ s$^{-1}$ (Fig. 5). Other studies (Borken et al., 1999; Kelliher et al., 1999; Pumpanen et al., 2003) have also found similar increase in $CO_2$ efflux following the increase in soil moisture after a dry period. This burst of $CO_2$ is probably due to two major factors: Firstly, large proportions of microorganisms die or become dormant during drought (van Gestel et al., 1991) and their dead cells decompose during rewetting. Secondly, during the drought, the soil organic matter, such as root and litter, accumulates on the soil; when rewetted, the

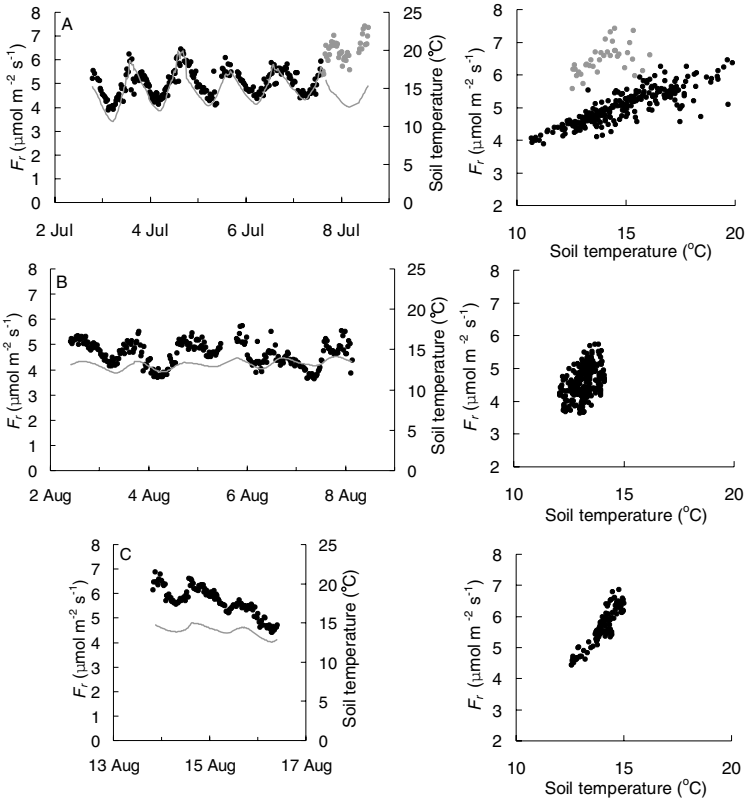


*Fig. 5.* Soil $CO_2$ flux and respiration of floor vegetation, $F_r$ ($\mu$mol m$^{-2}$ s$^{-1}$), measured with the darkened big chamber (black spheres) and soil temperature (°C, grey line). The different panels (A, B, C) correspond to the different measuring locations of the chamber. $F_r$ values measured at the first location after a rain shower at 7 July are marked with grey spheres. The right hand side shows the temperature dependence of $F_r$.

microbial population recovers and begins using the fresh organic matter. Thus, $F_r$ cannot be attributed solely to the soil temperature. These sorts of small and transient changes are very difficult to observe clearly in the EC or transparent chamber data (Fig. 4).

Rain fell intermittently during the second period; thus, we had no distinct dry period. During the period, the variation in $F_r$ is less well linked to soil temperature than during the first and third periods, apparently the result of large variations in soil moisture and water dynamics in the soil (see later, Fig. 7). In the third plot, $F_r$ decreased over time, as did the amplitude of the net forest floor $CO_2$ exchange (Fig. 4). The simultaneous significant decrease in $F_r$ (from ~7 to ~4.5 $\mu$mol m$^{-2}$ s$^{-1}$) may indicate that the carbon cycle of mosses is relatively fast and a large part of the assimilated $CO_2$ is released rapidly due to a lack of storage capacity. The assimilation rate depends on air temperature and radiation. During the third measuring period, the average daily radiation pattern remained substantially steady while air temperatures dropped from 14.5 °C to 10.8 °C which may have reduced the rate of assimilation, and thereby the rate of moss respiration as well. The decrease in $F_r$, however, can also be attributed to spatial variation in the temperature dependence of the soil $CO_2$ flux and to respiration of the vegetation (Fig. 5). Nevertheless, we need more careful measurements to uncover the true connection between assimilation and respiration.

*3.5.2. Measurements of gross photosynthesis over a community, $P_{ch}$.* The rate of gross photosynthesis measured with the big chamber was, at its peak, 6.5 $\mu$mol m$^{-2}$ s$^{-1}$ in the first measurement location, 4 $\mu$mol m$^{-2}$ s$^{-1}$ in the second and 4.5 $\mu$mol m$^{-2}$ s$^{-1}$ in the third location (Fig. 6). Due to technical problems, however, most of the gross photosynthesis measurements are missing from the second location during the daytime, when PAR was at its peak. Widén (2002) found the maximum gross photosynthesis rate of forest floor vegetation in a 50-year-old mixed stand to be 5.2 $\mu$mol m$^{-2}$ s$^{-1}$ when vegetation consisted of blueberry and mosses. Our momentary gross photosynthesis rates measured in blueberry-dominated location are in reasonable agreement with their results.

*3.5.3. Momentary photosynthesis of individual plant species.* The $P_{max}$ values fitted (eq. 3) for different plant species ranged from 0.008 $\mu$mol g$^{-1}$ s$^{-1}$ of mosses to 0.184 $\mu$mol g$^{-1}$ s$^{-1}$ of blueberry (Table 2). Blueberry, with its thin annual leaves, has a $P_{max}$ two to three times as high as that of heather or lingonberry, which have perennial leaves. The $P_{max}$ for blueberry was highest in the beginning of July, but fell by 30% by mid July (Fig. 7). In the beginning of July (1–16 July), the cumulative precipitation was only 8 mm, resulting in reduced soil moisture (Fig. 7.). This may explain the decrease in the photosynthetic activity ($P_{max}$) of blueberry. In addition, the $P_{max}$ values of mosses were considerably lower in the first half of July before the soil moisture increased. This phenomenon was discovered also by Skre and

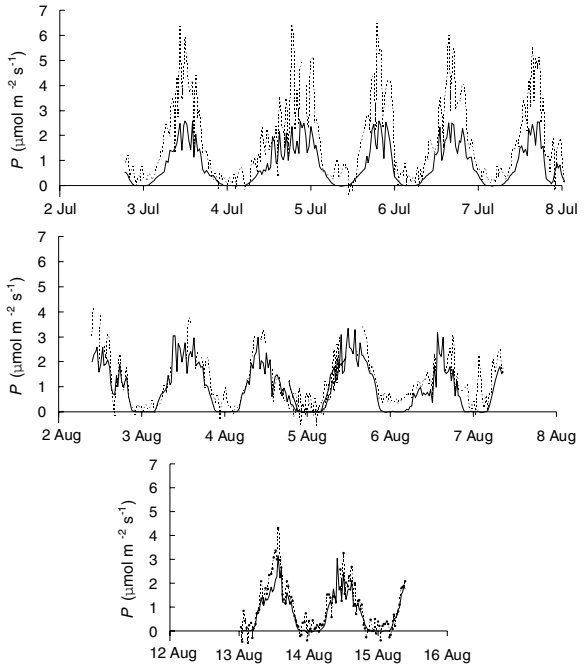


*Fig. 6.* Momentary rate of photosynthesis, $P$ ($\mu$mol m$^{-2}$ s$^{-1}$), by the big chamber measurements ($P_{ch}$, dashed line) and estimation with species-specific light response curves and average vegetation at the study site ($P_e$, black line). The different panels (A, B, C) correspond to the different measuring locations of the chamber.

*Table 2.* Species-specific parameter b ($\mu$mol m$^{-2}$ s$^{-1}$) and $P_{max}$ values ($\mu$mol g$^{-1}$ s$^{-1}$) in the light response curves (eq. 3) during the three measuring periods (2–9 Jul, 2–9 August, and 13–17 August 2005)

| | $B$ ($\mu$mol m$^{-2}$ s$^{-1}$) | $P_{max}$ ($\mu$mol g$^{-1}$ s$^{-1}$) | | |
|---|---|---|---|---|
| | | 1st | 2nd | 3rd |
| Blueberry | 109 | 0.184 | 0.139 | 0.132 |
| Lingonberry | 122 | 0.032 | 0.057 | 0.055 |
| Heather | 208 | 0.056 | 0.066 | 0.069 |
| Mosses | 10 | 0.008 | 0.014 | 0.015 |

Oechel (1981) and Williams and Flanagan (1998), who found that gross photosynthesis rates decrease with decreasing water content in the mosses.

The $P_{max}$ of blueberry failed to increase after the rain in the second half of July, unlike the $P_{max}$ of lingonberry (Fig. 7). Blueberry leaves are short-lived and become senescent early in the autumn, but according to Fig. 7, the drought in the first half of July may have hastened the decrease in $P_{max}$ or even caused permanent damage to the plants. However, to draw definite conclusions about the connection between the drought and the leaf damage will require more comprehensive and intensive measurements. The $P_{max}$ value for lingonberry was quite low at the beginning of

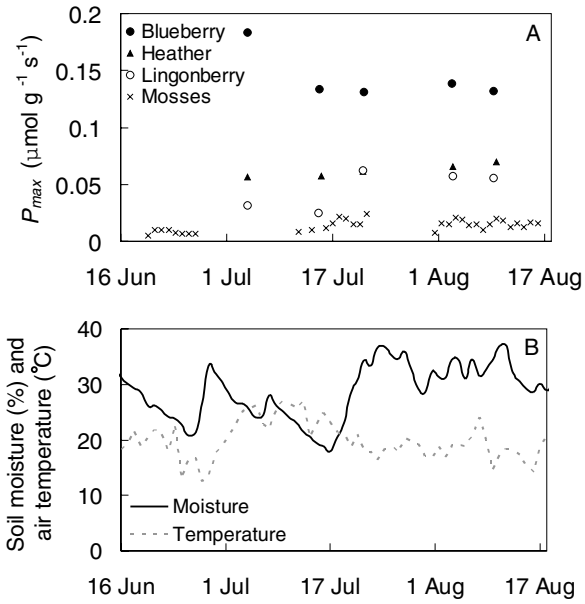


*Fig. 7.* Manually measured $P_{max}$ values for each species (A), and average daily soil moisture and air temperature readings (B) from 16 June to 17 August 2005.

July, and then nearly doubled when the soil was rewetted. This could, nevertheless, be coincidental, since the new leaves of lingonberries increase their photosynthetic capacity relatively late in the summer. Gerdol et al. (2000) found that the expansion of lingonberry leaves lasted for 3 months, whereas the expansion of blueberry leaves lasted only 3 weeks. The photosynthetic activity of heather seems to have no apparent connection to soil moisture in the prevailing conditions. Kolari et al. (2006) estimated the $P_{max}$ values to be 0.139, 0.033, 0.062 and 0.02 $\mu$mol g$^{-1}$ s$^{-1}$ for blueberry, lingonberry, heather and mosses, respectively. Their values all fall in the range of the values found in this study (Table 2), except for mosses, for which the $P_{max}$ values in this study are lower. Parameter $b$ values for the species studied in Kolari et al. (2006) were 146, 164, 240 and 21 $\mu$mol m$^{-2}$ s$^{-1}$, which are a bit higher than our values, but are still within the same range and relation to each other.

The momentary gross photosynthesis rates per ground area ($P_e$) estimated from the light response curves of individual plant species, measurements of PAR and the average leaf biomass in the study site (Table 1) are shown in Fig. 6. The maximum daily rates were between 2 and 3 $\mu$mol g$^{-1}$ s$^{-1}$ in all of the periods. Other studies (Subke and Tenhunen, 2004; Launiainen et al., 2005; Kolari et al., 2006) have reported similar results. In all three locations, $P_e$ was lower than the gross photosynthesis rates measured from the plant community in the big chamber ($P_{ch}$), particularly at the first location where $P_e$ reached a maximum of about 2.5 $\mu$mol m$^{-2}$ s$^{-1}$ while $P_{ch}$ had maximum values of about 6–7 $\mu$mol m$^{-2}$ s$^{-1}$ (Fig. 8). This is likely due to placement of the chamber in locations with no visible disturbance of the forest floor vegetation (i.e. the mass per unit ground area of the

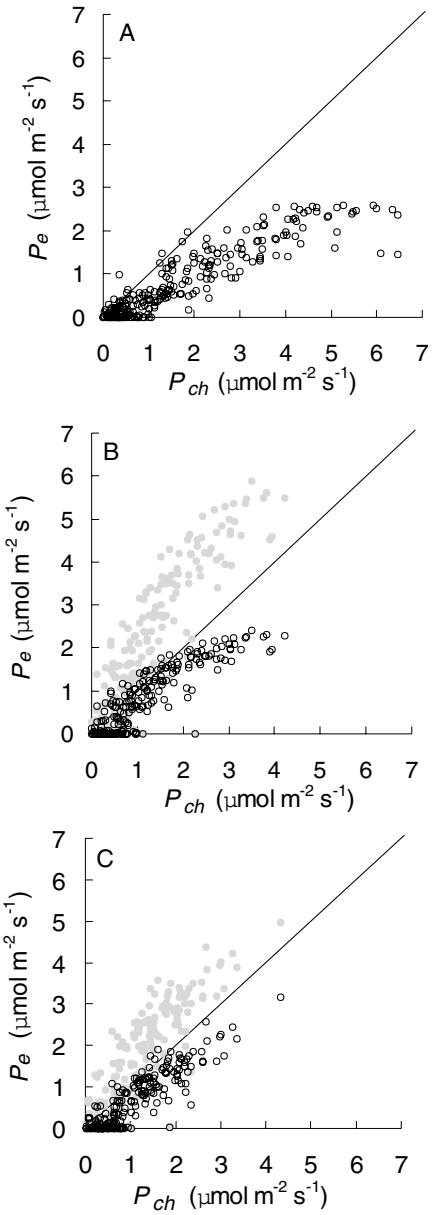


*Fig. 8.* Comparisons of the big chamber measurement ($P_{ch}$) and species-specific estimations ($P_e$): Estimation by the average vegetation at the study site (grey spheres) and estimation by vegetation in the big chamber (black circles). The different panels (A, B, C) correspond to the different measuring locations of the chamber. Precise information on the vegetation in the big chamber is missing from the first location. Consequently, only an estimation by the average vegetation is available.

respective species was higher in the chamber than on average, Table 1).

### *3.6. Comparison of the chamber methods*

The light response functions for the different species together with the measured PAR and the dry mass of the respective species within the big chamber allowed comparison of the gross photosynthesis measured over the whole plant community in the big chamber ($P_{ch}$) to the sum of the estimated gross photosynthesis of the respective species ($P_{e\_ch}$). The $P_{e\_ch}$ was generally higher than $P_{ch}$ in the second and third locations (Fig. 8) (leaf mass data missing for the first location). This overestimation is probably due to high self-shading (caused by the dense vegetation) which does occur in the chamber measurements. When $P_i$ was measured from individual shoots, they never shaded each other, whereas the shoots and leaves overlapped when the whole plant community was measured in the big chamber. In addition, the light response curves of mosses were measured with no shading from other vegetation. Moreover, the light intensities under the dense lingonberry population in the big chamber were probably very low. Shading by the chamber structure presumably also slightly decreases the rate of gross photosynthesis. Furthermore, the substrate in the light response measurements of mosses may also increase the difference between the results of different methods. The substrate in the light response measurements of mosses was possibly richer than in the big chamber, where the mosses had, for instance, less water available due to the presence of vascular plants. The difference in the habitats may have led to the small overestimation of $P_{e\_ch}$ also for the third plot (Fig. 8).

The comparison between these two methods, $P_{e\_ch}$ and $P_{ch}$, demonstrates the difficulties in upscaling. The results differ, even though the area over which the upscaling and measurement took place is relatively small and homogeneous. Different measuring methods should not, however, be considered exclusionary or competing approaches; rather, the aim of the study should guide. For instance, to estimate the gross photosynthesis of forest floor vegetation in different environmental conditions or in other areas than those near the measuring site requires detailed understanding of the underlying processes. Automatic chambers, especially those with a darkening feature, provide a very effective tool for this. The chambers yield precise results for the plot being measured. Consequently, they can successfully serve the study of environmental responses to the processes controlling $CO_2$ and $H_2O$ fluxes at the forest floor. In proportion, the measurements of the gross photosynthesis of individual species provide precise information on the photosynthetic capacity of a shoot and on the separate responses of different species. Therefore, shoot measurements are likely the most useful for model parameter development. On the other hand, because of the difficulties in upscaling, a large-scale method such as EC would be the choice if the aim is to achieve representative average values for $CO_2$ and $H_2O$ exchange.

## 4. Conclusions

According to our EC measurements, we found forest floor evapotranspiration to reach daily maximum of 1.5–2.0 mmol $m^{-2}\,s^{-1}$. Evapotranspiration measured with the chamber method depended heavily on the type of vegetation present.

Transpiration from a blueberry-dominated plot was greater than that from a lingonberry- or moss-dominated location. Diurnal amplitude in net $CO_2$ measurements was also strongly dependent on the photosynthesising vegetation within the chamber. The chambers gave higher diurnal amplitude (from ~4 to ~6 $\mu$mol $m^{-2}$ $s^{-1}$), than the EC measurements (from ~3 to ~4 $\mu$mol $m^{-2}$ $s^{-1}$), probably due to different vegetation density in the chambers. The chambers are usually placed on undisturbed soil surfaces with well-developed ground vegetation, although forest floors normally have unvegetated surfaces as well, such as pale rocks or logging waste, which influence the average areal net fluxes. Our chamber measurements also indicated spatial variation in net $CO_2$ flux, which depends heavily on soil temperature and soil moisture. The diurnal amplitudes of soil $CO_2$ efflux and the respiration of forest floor vegetation, $F_r$, varied from 1 to 2.5 $\mu$mol $m^{-2}$ $s^{-1}$, and depended on location and soil moisture.

The $P_{max}$ values of individual plant species varied from 0.008 (mosses) to 0.184 $\mu$mol $m^{-2}$ $s^{-1}$ (blueberry) depending on the phase of development and soil moisture. $P_{max}$ values decreased during a short drought – except for heather, which seemed to show no connection between soil moisture and the rate of photosynthesis. Using these $P_{max}$ values of individual plant species, defined per leaf mass, and values for average vegetation we obtained results for the areal rate of photosynthesis (2–3 $\mu$mol $m^{-2}$ $s^{-1}$) similar to those of other studies and EC measurements. However, upscaling with the light responses of individual plant species and leaf mass failed to yield results similar to measurements from the chamber with a dense community of different species. This was probably influence of significantly less shading and different substrate characteristics when the species-specific $P_{max}$ was measured. Therefore, upscaling from chambers should be considered carefully in studies that focus mainly on average net fluxes. Dense vegetation in chambers is a potential source of overestimation of gross photosynthesis if measurements are upscaled to a larger area. Similarly, uspcaling the measured soil respiration carries a risk for bias because, soil characteristics, such as its water-holding capacity, fertility, distance to trees and other growing conditions, such as light, vary spatially. Because soil characteristics and vegetation are usually heterogeneous, chambers are the most suitable for small-scale process studies for which EC may be too coarse because it measures the total ecosystem exchange.

## 5. Acknowledgments

This study was carried out within the framework of the Nordic Centre for Studies of Ecosystem Carbon Exchange and its Interaction with the Climate System (NECC), funded by the Nordic Centre of Excellence (NCoE), the Responses of boreal ecosystem carbon exchange to changing environments in different spatio-temporal scales (REBECCA) project of the Helsinki University Environmental Research Centre (HERC) and the CarboEurope. Monika Strömgren and Toivo Pohja are greatly acknowledged for their installations and technical assistance during the project.

## References

Aubinet, M., Grelle, A., Ibrom, A., Rannik, Ü., Monchrieff, J. and co-authors 2000. Estimates of the annual net carbon and water exchange of forests: the EUROFLUX Methodology. *Adv. Ecol. Res.* **30**, 113–178.

Baldocchi, D. D. 2003. Assessing the eddy covariance technique for evaluating carbon dioxide exchange rates of ecosystems: past, present and future. *Global. Change. Biol.* **9**, 479–492.

Baldocchi, D. D. and Vogel, C. A. 1996. Energy and $CO_2$ flux densities above and below a temperate broad-leaved forest and a boreal pine forest. *Tree. Physiol.* **16**, 5–16.

Baldocchi, D. D., Law, B. E. and Anthoni, P. M. 2000. On measuring and modeling energy fluxes above the floor of a homogenous and heterogeneous conifer forest. *Agric. For. Meteorol.* **102**, 187–206.

Blanken, P. D., Black, T. A., Neumann, H. H., Den Hartog, G., Yang, P. C. and co-authors 1998. Turbulent flux measurements above and below the overstory of a boreal aspen forest. *Boundary-Layer Meteorol.* **89**, 109–140.

Borken, W., Xu, Y.-J., Brumme, R. and Lamersdorf, N. 1999. A climate change scenario for carbon dioxide and dissolved organic carbon fluxes from a temperate forest soil: drought and rewetting effects. *Soil Sci. Soc. Am. J.* **63**, 1848–1855.

Cajander, A. K. 1926. The theory of forest types. *Acta For. Fen.* **29**, 1–108.

Constantin, J., Grelle, A., Ibrom, A. and Morgenstern, K. 1999. Flux partitioning between understorey and overstorey in a boreal spruce/pine forest determined by the eddy covariance method. *Agric. For. Meteorol.* **98–99**, 629–643.

Gerdol, R., Iacumin, P., Marchesini, R., Bragazza, L. 2000. Water- and nutrient-use efficiency of a deciduous species Vaccinium myrtillus, and evergreen species, V. Vitis-ideae, in a subalpine dwarf shrub heath in the Southern Alps, Italy. *Oikos* **88**, 19–32.

Goulden, M. L. and Crill, P. M. 1997. Automated measurements of $CO_2$ exchange at the moss surface of a black spruce forest. *Tree Physiol.* **17**, 537–542.

Goulden, M. L., Munger, J. W., Fan, S.-M., Daube, B. C. and Wofsy, S. C. 1996. Measurements of carbon sequestration by long-term eddy covariance: methods and a critical evaluation. *Global Change Biol.* **2**, 159–168.

Hari, P. and Kulmala, M. 2005. Station for measuring Ecosystem-Atmosphere Relations (SMEARII). *Bor. Env. Res.* **10**, 315–322.

Heijmans, M. M. P. D., Arp, W. J. and Chaplin III, F. S. 2004. Carbon dioxide and water vapour exchange from understory species in boreal forest. *Agric. For. Meteorol.* **123**, 135–147.

Janssens, I. A., Kowalski, A. S. and Ceulemans, R. 2001. Forest floor $CO_2$ fluxes estimated by eddy covariance and chamber-based model. *Agric. For. Meteorol.* **106**, 61–69.

Kelliher F. M., Lloyd J., Arneth A., Lühker B., Byers J. N. and co-authors. 1999. Carbon dioxide efflux density from the floor of a central Siberian pine forest. *Agric. For. Meteorol.* **94**, 217–232.

Kolari, P., Pumpanen, J., Kulmala, L., Ilvesniemi, H., Nikinmaa, E. and co-authors. 2006. Forest floor vegetation plays an important role in

photosynthetic production of boreal forests. *For. Ecol. Manage.* **221**, 241–248.

Launiainen, S., Rinne, J., Pumpanen, J., Kulmala, L., Kolari, P. and co-authors. 2005. Eddy covariance measurements of $CO_2$ and sensible and latent heat fluxes during a full year in a boreal pine forest trunk-space. *Bor. Env. Res.* **10**, 569–588.

Launiainen, S., Pumpanen, J., Mölder, M., Kulmala, L., Lankreijer, H. and co-authors. 2006. Vertical variations in fluxes and turbulence characteristics within a forest – a joint NECC-campaign in Hyytiälä, Southern Finland. In: *Proceeding of BACCI, NECC and FcoE activities 2005 book B*, *Report Series in Aerosol Sciences 81A* (eds. M. Kulmala, A. Lindroth and T. M. Ruuskanen), Helsinki, Finland.

Misson, L., Baldocci, D. D., Black, T. A., Blanken, P. D., Brunet, Y. and co-authors. H. 2007. Partitioning forest carbon fluxes with overstory and understory eddy-covariance measurements: a synthesis based on FLUXNET data. *Agric. For Meteorol.* **144**, 14–31.

Morén, A.-S. and Lindroth, A. 2000. CO2 exchange at the floor of a boreal forest. *Agric. For. Meteorol.* **101**, 1–14.

Pumpanen, J., Ilvesniemi, H., Keronen, P., Nissinen, A., Pohja, T. and co-authors. 2001. An open chamber system for measuring soil surface $CO_2$ efflux: analysis of error sources related to the chamber system. *J. Geophys. Res*. **106**, 7985–7992.

Pumpanen, J., Ilvesniemi, H., Peramaki, M. and Hari, P. 2003. Seasonal patterns of soil CO2 efflux and soil air CO2 concentration in a Scots pine forest: comparison of two chamber techniques. *Global Change Biol.* **9**, 371–382.

Skre, O. and Oechel, W. 1981. Moss functioning in different taiga ecosystems in interior Alaska. 1. Seasonal, Phenotypic, and drought effects on photosynthesis and response patterns. *Oecologia* **48**, 50–59.

Subke, J. A. and Tenhunen, J. D. 2004. Direct measurements of CO2 flux below a spruce forest canopy. *Agric. For. Meteorol.* **126**, 157–168.

Swanson, R.-V. and Flanagan, L.-B. 2001. Environmental regulation of carbon dioxide exchange at the forest floor in a boreal black spruce ecosystem. *Agric. For. Meteorol.* **108**(3), 165–181.

Valentini, R., Matteucci, G., Dolman, A. J., Schulze, E.-D., Rebmann, C. and co-authors.2000. Respiration as the main determinant of carbon balance in European forests. *Nature* **404**, 861–865.

Van Gestel, M., Ladd, J. N. and Amato, M. 1991. Carbon and nitrogen mineralization from two soils of contrasting texture and microaggregate stability: influence of sequential fumigation, drying and storage. *Soil Biol. Biochem*. **23**, 313–322.

Whitehead, D. and Gover, S. T. 2000. Photosynthesis and light-use efficiency by plants in a Canadian boreal forest ecosystem. *Tree Physiol.* **21**, 925–929.

Widén, B. 2002. Seasonal variation in forest-floor CO2 exchange in a Swedish coniferous forest. *Agric. For. Meteorol.* **111**, 283–297.

Williams, T. G. and Flanagan, L. B. 1998. Measuring and modelling environmental influences on photosynthetic gas exchange in Sphagnum and Pleurozium. *Plant Cell Env.* **21**, 555–564.

Wilson, K. B. and Meyers, T. P. 2001. The spatial variability of energy and carbon dioxide fluxes at the floor of a deciduous forest. *Boundary-Layer Meteorol.* **98**(3), 443–473.